Accepted Manuscript

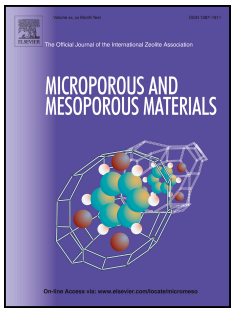

Jute-derived microporous/mesoporous carbon with ultra-high surface area using a chemical activation process

Junayet Hossain Khan, Freddy Marpaung, Christine Young, Jianjian Lin, Md Tofazzal Islam, Saad M. Alsheri, Tansir Ahamad, Norah Alhokbany, Katsuhiko Ariga, Lok Kumar Shrestha, Yusuke Yamauchi, Kevin C.-W. Wu, Md Shahriar A. Hossain, Jeonghun Kim

PII: S1387-1811(18)30424-4

DOI: 10.1016/j.micromeso.2018.07.050

Reference: MICMAT 9060

To appear in: *Microporous and Mesoporous Materials*

Received Date: 10 June 2018

Revised Date: 24 July 2018

Accepted Date: 30 July 2018

Please cite this article as: J.H. Khan, F. Marpaung, C. Young, J. Lin, M.T. Islam, S.M. Alsheri, T. Ahamad, N. Alhokbany, K. Ariga, L.K. Shrestha, Y. Yamauchi, K. C.-W. Wu, M.S.A. Hossain, J. Kim, Jute-derived microporous/mesoporous carbon with ultra-high surface area using a chemical activation process, *Microporous and Mesoporous Materials* (2018), doi: 10.1016/j.micromeso.2018.07.050.

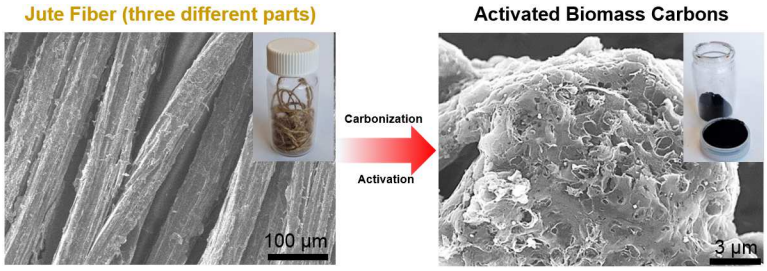

Jute-Derived Microporous/Mesoporous Carbon with Ultra-High Surface Area Using a Chemical Activation Process

Junayet Hossain Khan[+1,2], Freddy Marpaung[+2], Christine Young[3], Jianjian Lin[1], Md. Tofazzal Islam[4], Saad M. Alsheri[5], Tansir Ahamad[5], Norah Alhokbany[5], Katsuhiko Ariga[3], Lok Kumar Shrestha[3], Yusuke Yamauchi[6,7], Kevin C.-W. Wu[8], Md. Shahriar A. Hossain*[6] and Jeonghun Kim*[6]

[1] College of Chemistry and Molecular Engineering, Qingdao University of Science and Technology, Qingdao 266042, China

[2] Australian Institute for Innovative Materials (AIIM), University of Wollongong, Squires Way, North Wollongong, NSW 2500, Australia

[3] International Center for Materials Nanoarchitectonics (WPI-MANA), National Institute for Materials Science (NIMS), 1-1 Namiki, Tsukuba, Ibaraki 305-0044, Japan

[4] Department of Biotechnology, Bangabandhu Sheikh Mujibur Rahman Agricultural University, Gazipur 1706, Bangladesh

[5] Department of Chemistry, College of Science, King Saud University, Riyadh 11451, Saudi Arabia

[6] School of Chemical Engineering, School of Mechanical & Mining Engineering, and Australian Institute for Bioengineering and Nanotechnology (AIBN), The University of Queensland, Brisbane, QLD 4072, Australia

[7] Department of Plant and Environmental New Resources, Kyung Hee University, 1732 Deogyeong-daero, Giheung-gu, Yongin-si, Gyeonggi-do 446-701, South Korea

[8] Department of Chemical Engineering, National Taiwan University. No. 1, Sec. 4, Roosevelt Road, Taipei 10607, Taiwan

[+] These authors contributed equally to this work.

E-mails: md.hossain@uq.edu.au; jeonghun.kim@uq.edu.au

Keywords: Jute; biomass; nanoporous carbons; porous materials; adsorbents; graphitization

Abstract

Here, we report the synthesis of nanoporous carbons (NCs) derived from a low-cost and renewable biomass, jute, by a chemical activation process using KOH. Jute is one of the least expensive and most abundant crops, with a staggering 2.8 million metric tons of jute produced each year. In this study, we synthesize NCs from three different parts of jute fibers through a chemical activation technique using KOH. The NCs prepared from the bottom portion of the fiber show a high surface area (2682 $m^2 \cdot g^{-1}$) with the presence of both micropores and mesopores. The ultra-high surface area of jute makes it an economically viable, environmentally friendly precursor for NCs, with a wide variety of applications from energy storage to environmental and biomedical applications.

Introduction

There has been relentless effort and a persistent desire to synthesize new porous materials with novel characteristics and exciting applications. The reason for such interest and development is the potential to obtain high surface area, tunable pore size, functional site availability, and guest-host interactions that can be used in a wide variety of fields, such as the biomedical and energy sectors, and for promising applications, for example, as adsorbents and catalysts.[1-2] Among the many porous materials, nanoporous carbons (NCs), with interpenetrating and regular nanopore systems, have recently inspired great research activity because of their fascinating chemical and physical properties, such as high specific surface area, well-defined pore structure, high thermal and chemical stability, intrinsic high electrical conductivity, low density and wide availability.[3-5] Therefore, NCs have been implemented in hydrogen storage,[6] pollutant adsorption,[7] energy storage,[8] energy conversion[9] and electrochemical sensing.[10] Recently, many research efforts have been devoted to carbon synthesis through the improvement of existing fabrication methods, as well as the development of new approaches. Nanoporous materials can be generally classified based on their pore diameter. Accordingly, free pore diameters less than 2 nm are classified as micropores, those between 2 nm and 50 nm are classified as mesopores, and pore sizes greater than 50 nm fall under macropores.[11] Conventional porous carbon materials, such as activated carbon, are routinely prepared by pyrolysis[12] or hydrothermal treatment[13] followed by chemical[14] or physical[15] activation of the organic precursors. However, the realization of ultra-high surface areas beyond the 2500 $m^2 \cdot g^{-1}$ threshold of NCs using waste biomass precursors via facile routes with the use of only oxidizing agents and heat treatment is a major challenge for researchers.[16]

Recently, biomass-derived porous carbons have attracted the attention of researchers for use in a wide range of applications. Biomass-derived porous carbon is not only environmentally friendly but also cost effective, and the ease of availability makes it a promising precursor compared with its competitors.[17-19] Biomass refers to plant, plant-derived, animal-derived, industrial-derived, or sewage- or municipal waste-derived materials that can be utilized to synthesize carbon materials for a variety of applications.[20] Currently, the most common precursors used to synthesize various porous carbon materials are cherry stones,[21] coffee

husks,[22] banana peels,[23] almond shells,[24] corn cobs,[25] cotton stalks,[26] dates stones,[27] olive stones,[28] rice bran,[29] rice husks,[30] rice straw,[31] rice hulls,[32] sugarcane bagasse,[33] sawdust,[34] tea waste,[35] walnut shells,[36] durian shells,[37] herb residues,[38] waste apricot,[39] orange peels,[40] oil palm fibers,[41] coconut husks[42], etc. In addition, activated porous biocarbons using single-step activation have been reported.[43-46]

However, considering the limited research utilizing jute biomass, the surface area is confined between 400-1000 $m^2 \cdot g^{-1}$ for physically activated carbon[47,48] and 800-1200 $m^2 \cdot g^{-1}$ for chemically activated carbon[49,50]. Therefore, chemical activation generally results in a higher surface area than physical activation. With the ever-increasing demand for ultra-high-surface-area NC for applications such as energy storage, there is a need for cost-effective synthesis methods using renewable precursors that are scalable for commercial applications.

Here, we report the synthesis of NC derived from jute, a low-cost and renewable biomass, by a chemical activation process using KOH. Jute is one of the least expensive and most abundant crops, with a staggering 2.8 million metric tons of jute produced each year.[51] However, due to technology advancements, synthetic fibers started to dominate the fiber market due to their high production output, greater tensile strength and environmentally non-degradable properties. These synthetic fibers possess a significant risk to the environment because they are not decomposed like natural fibers over time. On the other hand, natural fibers such as jute are environmentally friendly not only because they decompose over time but also because have a great impact on the greenhouse effect. It has been estimated that one hectare of jute plants can absorb approximately 15 metric tons of CO_2 and release 11 metric tons of O_2 in just 120 days of the jute growing period.[52] A jute plantation of hundreds or thousands of hectares would greatly reduce the level of greenhouse gas in the atmosphere and increase the level of pure oxygen in the atmosphere. Transforming this inexpensive and abundant crop into useful and valuable NC materials could restore the livelihood of millions of people across Asia and Africa. Research into practical applications that use high-surface-area NC is the way ahead to solving many of the world's current problems. Very few reports have highlighted the conversion of jute fiber into valuable activated carbon using easy, inexpensive and scalable synthesis techniques.[47-50] At the same time reports on the

implementation of jute-derived high-surface-area NC using chemical activation are scarce. Additionally, the maximum surface area generated using jute- and jute-related precursors is less than 1200 $m^2 \cdot g^{-1}$.[50]

In this study, we synthesized NCs from three different parts of jute fibers through a chemical activation method using KOH. Nitrogen adsorption-desorption isotherms, X-ray diffraction (XRD), X-ray photoelectron spectroscopy (XPS), Raman spectroscopy, Fourier transform infrared (FTIR) spectroscopy, UV spectroscopy, and scanning/transmission electron microscopy (SEM/TEM) were performed to characterize the morphology and porous structure of the obtained NCs. The NC prepared from the bottom portion of the fiber showed a high surface area (2682 $m^2 \cdot g^{-1}$) with the presence of both micropores and mesopores. The ultra-high surface area of jute-derived carbon makes jute an economically viable, environmentally friendly precursor for NCs, with a wide variety of applications from energy storage to environmental and biomedical applications.

Experimental

Preparation of nanoporous activated carbon. According to a previous report,[51] jute biomass contains a high quantity of carbon in the form of pentosan (20-23 wt%), cellulose (45-48 wt%), and lignin (12-15 wt%). Furthermore, the jute biomass used in this work has a very low ash level (1-2 wt%) compared to rice husk (17-18 wt%), bagasse (3-4 wt%), and wheat straw (13-14 wt%) raw biomass. The jute fibers (~190 cm) were cut and divided into three parts: bottom (70 cm), middle (70 cm), and top (rest 50 cm) parts. Each part was then cut into smaller pieces (~5 cm) and washed with warm distilled water(~50 °C) several times (15 times) and finally dried at 100 °C for 4 h. **As shown in Scheme 1,** the dried jute fibers were then pre-carbonized at 300 °C for 12 h under air atmosphere and finally allowed to cool to room temperature by areal cooling. The pre-carbonized samples were then crushed into powder. The powder sample was mixed with KOH (1:1 wt ratio) and ground in an agate mortar until well mixed and a paste-like form was achieved. The mixture was stored at room temperature for 12 h before carbonization. The carbonization was carried out in a tubular furnace (KOYO-Japan) at 900 °C for 3 h under a constant flow of nitrogen (120 cc min^{-1}) at a heating ramp of 5 °C min^{-1}. After carbonization, the samples were washed with dilute HCl (0.1 M) and water to remove any leftover potassium/inorganic residues and finally vacuum dried at 80 °C for 12 h. The carbon samples obtained from the bottom, middle and top parts are referred to as J-B, J-M and J-T, respectively.

Characterization. Wide-angle XRD patterns were acquired using a Rigaku RINT 2500X diffractometer using monochromated Cu Kα radiation (40 kV, 40 mA) at a scanning rate of 2°·min^{-1}. The morphology and microstructure were investigated via SEM and TEM. A Hitachi S-4800 SEM was used to obtain the SEM images at an accelerating voltage of 5 kV. A JEM-2010 TEM was utilized to perform the TEM observations at 200 kV. Raman spectra were measured using a Raman JY HR800 spectrometer. FTIR spectroscopy was performed using a Shimadzu FTIR Prestige-21. Textural characterization was carried out by collecting nitrogen adsorption-desorption isotherms using a Quantachrome Autosorb Automated Gas sorption system at 77 K. UV-3600 and UV-VIS-NIR spectrophotometers were used to evaluate the adsorption of methylene blue (MB).

Results and discussion

Figure 1 shows the SEM images of natural jute and jute-derived NCs using different parts of the jute fiber. **Figure 1a** shows the strand-like framework of the natural jute fibers. After pre-carbonization followed by chemical activation prior to impregnation *via* KOH, activated NCs were obtained (**Figure 1b-d**). After treatment, the original fibrous structure was permanently changed to a globular shape.

Figure 2a shows the wide-angle XRD patterns of the jute-derived NCs obtained from three different parts of the jute fiber (bottom, middle, and top parts). One broad peak at 2θ = 20-25°, which corresponds to the (002) plane of the graphitic structure, was observed.[52,53] All the carbon samples, regardless of the part of the jute fiber used, exhibited broad peaks, suggesting the formation of poorly graphitized carbon. Raman spectroscopy further confirms the presence of graphitic carbon. As shown in **Figure 2b**, two broad peaks are observed at 1353 cm^{-1} and 1597 cm^{-1}, which correspond to the previously reported D and G bands.[54,55] The D band relates to the disordered carbon phase, whereas the G band relates to the sp^2-hybridized graphite phase. The relative intensity ratios of the D band to the G band (I_D/I_G) are 1.25, 0.83, and 1.05 for J-B, J-M, and J-T, respectively. In our previous research, we directly carbonized jute and investigated the Raman spectrum.[51] In this case, with an increase in applied temperature, the I_D/I_G ratio gradually increases, indicating the generation of a larger number of defects. The I_D/I_G ratios are 0.96 (for 700 °C), 1.16 (for 800 °C), and 1.26 (for 900 °C). These values are much lower than that of commercially available activated carbon (2.06). Although in the present study we subjected the jute-derived carbon to an activation process, the low I_D/I_G ratio remained. The carbon sample prepared from the middle part of jute (J-M) shows the lowest value, indicating a higher graphitic degree. The N_2 adsorption-desorption isotherms of the different samples are presented in **Figure 3a**.

The instantaneous increase in adsorption at very low relative pressure indicates the presence of micropores. The subsequent gradual increase in the isotherm with increasing relative pressure suggests the presence of mesopores of various pore sizes. The non-localized density functional theory (NLDFT) method was utilized to obtain the pore size distribution shown in **Figure 3b**, which highlights the presence of both micropores and mesopores in all three samples. The J-B shows the highest portion of micropores comparing to

those of J-T and J-M. The surface areas of the three samples were calculated by the Brunauer-Emmett-Teller (BET) method and were found to be 2682 $m^2 \cdot g^{-1}$ (for J-B), 1909 $m^2 \cdot g^{-1}$ (for J-M), and 2494 $m^2 \cdot g^{-1}$ (for J-T). These values are higher than those of commercial activated carbon (1000-2000 $m^2 \cdot g^{-1}$) and significantly greater than other carbon materials prepared using plants.[51,56-58] The graphitic degree is in the order of J-M > J-T > J-B, while the surface area is in the order of J-B > J-T > J-M. The presence of many micropores greatly contributes to the increase in surface area. As seen in the low relative pressure region in **Figure 3a**, the amount of micropores decreases when the graphitization degree is high. This can be expected because the formation of micropores necessitates abundant sp^3-bonded carbons, which are mostly replaced by sp^2-bonds during the graphitization process.[59] Generally, the porosity and contents of hemicellulose, lignin, and cellulose of jute fibers differ by location.[60] It has been reported that middle portion of jute has less hemicellulose and lignin than top and bottom portions.[60,61] The hemicellulose and lignin have a less thermal stability than crystalline cellulose,[62] which can cause the collapse of pores in high temperature carbonization process. This fact likely causes the differences in surface area and graphitic degree in the final products.

Figure 4a shows the XPS survey spectrum of the J-B sample, indicating the presence of O and C elements in the sample. The deconvoluted C 1s spectrum (**Figure 4b**) has three distinct peaks at 288.3, 286.0, and 284.2 eV, corresponding to the oxygenated carbon species C=O, C–OH, and C=C/C–C, respectively. The highly intense C=C/C-C bonds indicate the good conducting nature of jute carbon through delocalized π electrons. In addition, the peaks indicated the presence of oxygen-containing groups due to the decomposition of jute cellulose, which contains oxygen; this has been observed previously in biomass-derived carbon materials.[63]

To investigate the implementation of ultra-high-surface-area NC for practical applications, such as water purification and toxin removal from aqueous media, we investigated the adsorption of MB by NC with dimensions of 1.43 nm × 0.61 nm × 0.4 nm (**Figure 5**). The adsorption capacity of commercially available carbon was also investigated. The maximum adsorption capacity of MB was determined by mixing MB solutions (50 ml) of different concentrations with carbon samples (10 mg) in the dark at 25 °C for 3 h until

equilibrium was established. The suspension was then centrifuged to separate the carbon samples from the solution. The supernatant solution was extracted using a syringe, and the concentration of MB was calculated by measuring the absorbance at 664 nm (maximum absorbance for MB). Finally, the amount of MB adsorbed by the carbon samples was calculated by deducting the MB concentration in the final solution from the initial MB concentration.

$Qe = (C_0\text{-}C_e)\cdot V\cdot m^{-1}$

where C_0 is the initial MB concentration in the liquid phase ($mg\cdot L^{-1}$), C_e is the MB concentration in the final solution ($mg\cdot L^{-1}$), V is the volume of solution used (L), and m is the mass of adsorbent used (g).

Jute-derived activated carbon exhibits a much higher adsorption capacity (> 200 $mg\cdot g^{-1}$) than expensive commercial activated carbon (176 $mg\cdot g^{-1}$).[51] The carbon sample prepared from the top part of the jute fiber shows the highest adsorption capacity of 239 mg g^{-1}. The high porosity and open pore network of the carbon matrix can facilitate fast molecular diffusion and promote accessibility to the entire pore surface. Interestingly, the MB adsorption capacity was normalized by the surface area obtained from the N_2 adsorption-desorption isotherm. The values are 0.078 $mg\cdot m^{-2}$ (for J-B), 0.115 $mg\cdot m^{-2}$ (for J-M), and 0.096 $mg\cdot m^{-2}$ (for J-T). As mentioned above, the graphitic degree is in the order of J-M > J-T > J-B. Thus, the MB dye more effectively interacted with the carbon surface due to π-π interactions between the MB molecule and graphitic carbon (sp^2-bonded carbon).[64]

Conclusion

Biomass-derived activated NCs were synthesized from jute fibers through pre-carbonization and chemical activation processes using KOH. Three different parts of the jute fiber were subjected to the chemical activation technique using KOH, and their porous properties were compared. The prepared NCs showed high surface areas of 2682 $m^2 \cdot g^{-1}$ (for J-B), 1909 $m^2 \cdot g^{-1}$ (for J-M), and 2494 $m^2 \cdot g^{-1}$ (for J-T). The highly increased surface area is attributed to the formation of both micropores and mesopores. In the MB adsorption test, J-T exhibited a high adsorption capacity of 239 $mg \cdot g^{-1}$. We believe that economically viable and environmentally friendly jute biomass is a promising material for the synthesis of carbon with ultra-high surface area for use in various applications, such as environmental and electrochemical storage applications.

Acknowledgement

This work was supported by the Australian Research Council (ARC) Future Fellow (grant FT150100479), JSPS KAKENHI (grants 17H05393 and 17K19044), and the research fund from the Suzuken Memorial Foundation. The authors extend their appreciation to the International Scientific Partnership Program (ISPP) at King Saud University (KSU) for funding this research work.

Reference

1. J. B. Fan, C. Huang, L. Jiang, and S. Wang, J. Mater. Chem. B, 2013, 1, 2222-2235.
2. M. H. Sun, S. H. Huang, L. H. Chen, Y. Li, X. Y. Yang, Z. Y. Yuan, and B. L. Su, Chem. Soc. Rev., 2016, 45, 3479-3563.
3. W. Xin, and Y. Song, RSC Adv., 2015, 5, 83239.
4. P. Srinivasu, A. Islam, S. P. Singh, L. Han, M. L. Kantam, and S. K. Bhargava, J. Mater. Chem., 2012, 22, 20866.
5. Y. Xia, Z. Yang, and R. Mokaya, Nanoscale, 2009, 2, 639-659.
6. Y. Xia, Z. Yang, and Y. Zhu, J. Mater. Chem A, 2013, 1, 9365.
7. P. Kowalczyk, J. Miyawaki, Y. Azuma, S. H. Yoon, K. Nakabayashi, P. A. Gauden, S. Furmaniak, A. P. Terzyk, M. Wisniewski, J. Wloch, K. Kaneko, and A. V. Neimark, Carbon, 2017, 124, 152-160.
8. S. Imtiaz, J. Zhang, Z. A. Zafar, S. Ji, T. Huang, J. A. Anderson, Z. Zhang, and Y. Huang, Scientific China Mater., 2016, 59(5), 389-407
9. S. Gao, K. Geng, H. Liu, X. Wei, M. Zhang, P. Wang, and J. Wang, Energy Environ. Sci., 2015, 8, 221.
10. L. Wang, Q. Zhang, S. Chen, F. Xu, S. Chen, F. Xu, S. Chen, J. Jia, H. Tan, H. Hao, and Y. Song, Anal. Chem., 2014, 86, 1414-1421.
11. B. D. Zdravkov, J. J. Cermak, M. Sefara, and J. Janku, Cent. Eur. J. Chem., 5(2), 385-395.
12. L. Bi, S. Ci, P. Cai, H. Li, and Z. Wen, App. Surf. Sci., 2018, 427, 10-16.
13. A. Jain, R. Balasubramanian, and M. P. Srinivasan, Chem. Eng. J., 2016, 283, 789-805.
14. F. Qi, Z. Xia, W. Wei, H. Sun, S. Wang, and G. Sun, Electrochimica Acta, 2017, 246, 59-67.
15. S. Rezma, M. Birot, A. Hafiane, and H. Deleuze, Comptes Rendus Chimie, 2017, 20, 881-887.
16. J. Deng, M. Li, and Y. Wang, Green Chem., 2016, 18, 4824.
17. Z. Gao, Y. Zhang, N. Song, and X. Li, Mater. Res. Lett., 2017, 5, 69-88.
18. M. M. Titirici, R. J. White, C. Falco, and M. Sevilla, Energy Environ. Sci., 2012, 5, 6796.
19. S. Dutta, J. Kim, Y. Ide, J. H. Kim, M. S. A Hossain, Y. Bando, Y. Yamauchi, K. C.-W. Wu, *Mater. Horiz.*, 4, 2017, 522-545.
20. J. Wang, P. Nie, B. Ding, S. Dong, X. Hao, H. Dua, and X. Zhang, J. Mater. Chem. A, 2017, 5, 2411-2428.
21. J. M. González-Domínguez, M. Alexandre-Franco, C. Fernández-González, A. Ansón-Casaos and V. Gómez-Serrano, J. Wood Chem. and Tech., 2017, 37, 148-162,
22. M. Gonclaves, M. C. Guerreiro, L. C. A. Oliveira, C. Solar, M. Nazarro, and K. Sapag, Waste Biomass Valor, 2013, 4, 395–400.

23. A. Borhan, S. Thangamuthu, M. F. Taha, and A. N. Ramdan, AIP Conference Proceedings, 2014, 1674, 020002.
24. D. Mohan, A. Sarswat, V. K. Singh, M. Alexandre-Franco, and C. U. P. Jr, Chem. Eng. J., 2011, 172, 1111-1125.
25. S. Nethaji, A. Sivasamy, and A. B. Mandal, Bioresource Tech., 2013, 134, 94-100.
26. M. Chen, X. Kang, T. Wumaier, J. Dou, B. Gao, Y. Han, G. Xu, Z. Liu, and L. Zhang, Journal of solid State
27. C. Bouchelta, M. S. Medjram, O. Bertrand, and J. P. Bellat, J. Anal. Appl. Pyrolysis, 2008, 82, 70-77.
28. I. Ghouma, M. Jeguirim, S. Dorge, L. Limousy, C. M. Ghimbeu, and A. Quederni, Comptes Rendus Chimie, 2015, 18, 63-74.
29. R. M. Suzuki, A. D. Andrade, J. C. Sousa, and M. C. Rollemberg, Bioresource Tech., 2006, 98, 1985-1991.
30. K. L. Van, and T. T. L. Thi, Progress in Natural Science: Materials International, 2014, 24, 191-198.
31. P. Gao, Z. –H. Liu, G. Xue, B. Hand, and M. –H. Zhaou, Bioresource Tech., 2011, 102, 3645-3648.
32. T. Mukoko, M. Mupa, U. Guyo, and F. Dziike, J. Environ. Anal. Toxicol. 2015, S7, 008.
33. K. Y. Foo, L. K. Lee, and B. H. Hameed, Bioresource Technology, 2013, 134, 166-172
34. M. A. F. Mazlam, Y. Uemura, S. Yusup, F. Elhassan, A. Uddin, and M. Demiya, Procedia Engineering, 2016, 148, 530-537.
35. M. Auta, and B. H. Hameed, Chem. Eng. J., 2011, 171, 502-509.
36. J. –W. Kim, M. –H. Sohn, D. –S. Kim, S. –M. Sohn, and Y. –S. Kwon, J. Hazard. Mater., 2001, B85, 301-315.
37. T. C. Chandra, M. M. Mirna, J. Sunarso, Y. Sudaryanto, and S. Ismadji, J. Taiwan Inst. Chem. Eng., 2009, 40, 457-462.
38. T. Mi, L. Chen, S. -Z, Xin, and X. –M, Yu, J. Nanomater., 2015, 8, 321-333.
39. C. A. Basar, J. Hazard. Mater., 2006, B135, 232-241.
40. M. E. Fernandez, G. V.Nunell, P. R. Bonelli, and A. L. Cikierman, Industrial Crops and Products, 2014, 62, 437-445.
41. A. R. Hidayu, N. F. Mohammad, S. Matali, and A. S. A. K. Sharifah, Procedia Engineering, 2013, 68, 379-384.
42. I. A. W. Tan, A. L. Ahmad, and B. H. Hameed, J. Hazard. Mater., 2007, 153, 709-717.
43. G. Singh, K. S. Lakhi, D.□H. Park, P. Srivastava, R. Naidu, and A. Vinu, *ChemNanoMat*, 2018, 4, 281-290.
44. Gurwinder Singh, In Young Kim, K. S. Lakhi, S. Joseph, P. Srivastava, R. Naidu, and A. Vinu, *J. Mater. Chem. A*, 2017, 5, 21196-21204.

45. G. Singh, K. S. Lakhi, K. Ramadass, S. Kim, D. Stockdale, A. Vinu, *Microporous Mesoporous Mater.*, 2018, 271, 23-32.
46. Gurwinder Singh, Kripal S. Lakhi, In Young Kim, Sungho Kim, Prashant Srivastava, Ravi Naidu, and Ajayan Vinu, *ACS Appl. Mater. Interfaces*, 2017, 9, 29782-29793.
47. M. Asadullah, M. A. Rahman, M. A. Motin, and M. B. Sultan, J. Surf. Sci. Tech., 2007, 23(1-2), 73-80.
48. C. Rombaldo, A. Lisboa, M. Mendez, and A. Coutinho, Anais da Academia Brasileira de Ciencais, 2014, 86(4), 2137-2144.
49. N. H. Phan, S. Rio, C. Faur, L. Coq, P. L. Cloirec, and T. H. Nguyen, Carbon, 2006, 44, 2569-2577.
50. T. Ramesh, N. Rajalakshmi, and K. S. Dhathathreyan, Energy Environ. Sustain., 2017, 2, 8.
51. J. H. Khan, J. Lin, C. Young, B. M. Matsagar, K. C. W. Wu, P. L. Dhepe, M. T. Islam, M. Rahman, L. K. Shrestha, S. M. Alshehri, T. Ahamad, R. R. Salunkhe, N. A. Kumar, D. J. Martin, Y. Yamauchi and M. S. A. Hossain, Mater. Chem. Phys, 2018, in press.
52. Q. Liang, L. Ye, Z.-H. Huang, Q. Xu, Y. Bai, F. Kang, Q.-H. Yang, Nanoscale, 6 (2014) 13831-13837.
53. J. Kim, C. Young, J. Lee, M.-S. Park, M. Shahabuddin, Y. Yamauchi, and J. H. Kim, Chem. Commun., 2016, 52, 13016-13019.
54. J. Kim, C. Young, J. Lee, Y.-U. Heo, M.-S. Park, M. S. A. Hossain, Y. Yamauchi, and J. H. Kim, J. Mater. Chem. A, 2017, 5, 15065-15072.
55. Y. Wang, D. C. Alsmeyer, and R. L. McCreery, Chem. Mater., 1990, 2, 557-563.
56. M.A. Islam, M.J. Ahmed, W.A. Khanday, M. Asif, B.H. Hameed, J. Environ. Manage., 2017, 203, 237-244.
57. P. Nowicki, J. Kazmierczak-Razna, R. Pietrzak, Mater. Des., 2016, 90, 579-585.
58. A. Reffas, V. Bernardet, B. David, L. Reinert, M.B. Lehocine, M. Dubois, N. Batisse, L. Duclaux, J. Hazard. Mater., 2010, 175, 779-788.
59. C. Young, R. R. Salunkhe, J. Tang, C.-C. Hu, M. Shahabuddin, E. Yanmaz, M. S. A. Hossain, J. H. Kim, and Y. Yamauchi, Phys. Chem. Chem. Phys., 2016, 18, 29308-29315.
60. S. Shahinur, M. Hasan, Q. Ahsan, D. K. Saha, and M. S. Islam, Inter. J. polymer Science, 2015, 262348, 6.
61. M. M. Kabir, Effects of chemical treatment on hemp fiber reinforced polyester composites, University of Southern Queensland, Toowoomba, Australia, 2012
62. A. Fardausy, M. A. Kabir, H. Kabir, H. Kabir, M. M. Rahman, K. Begam, F. Ahmed, M. A. Hossain, M. A. Gafur, Inter. J. Adv. Rese. Eng. Tech., 2012, 3, 267–274.
63. M. Baysal, K. Bilge, B. Yılmaz, M. Papila Y. Yürüm, J. Environ. Chem. Eng., 2018, 6, 1702-1713.

64. N.L. Torad, M. Hu, S. Ishihara, H. Sukegawa, A.A. Belik, M. Imura, K. Ariga, Y. Sakka, Y. Yamauchi, Small, 2014, 10, 2096-2107.

Figure legends

Figure legends

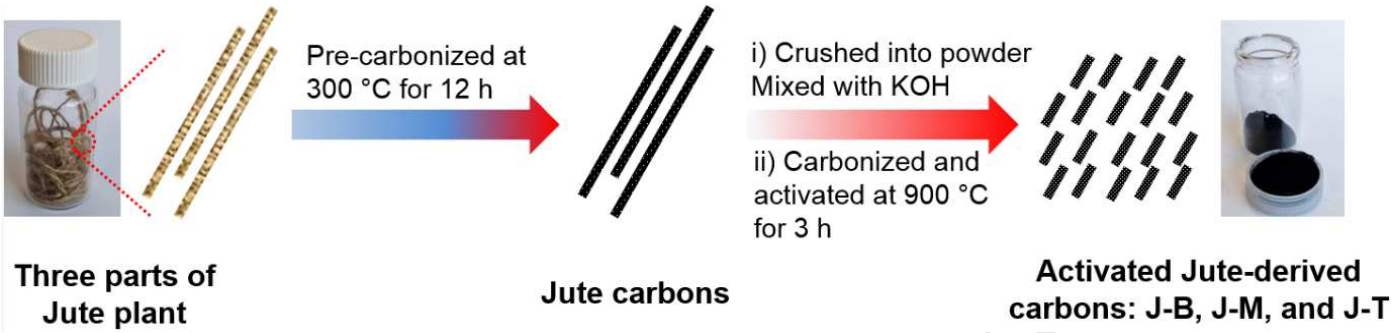

Scheme 1. Schematic illustration of the preparation of activated jute-derived nanoporous carbons.

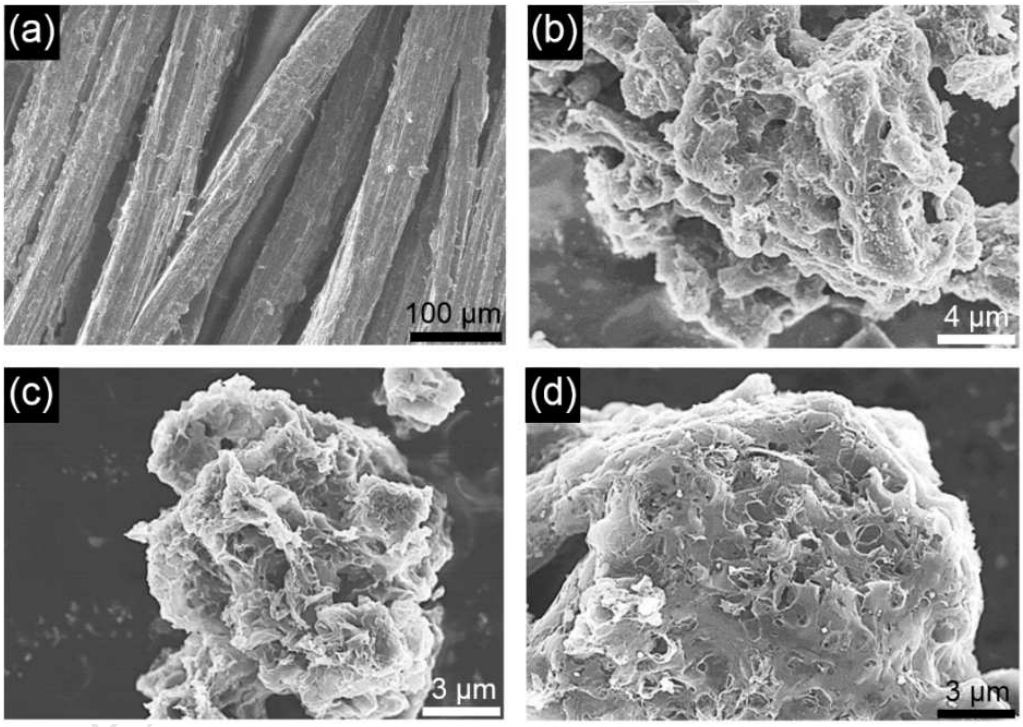

Figure 1. SEM images of (a) the jute fiber starting material and the activated nanoporous carbons (b) J-B, (c) J-M, and (d) J-T prepared from three different parts of the jute fiber.

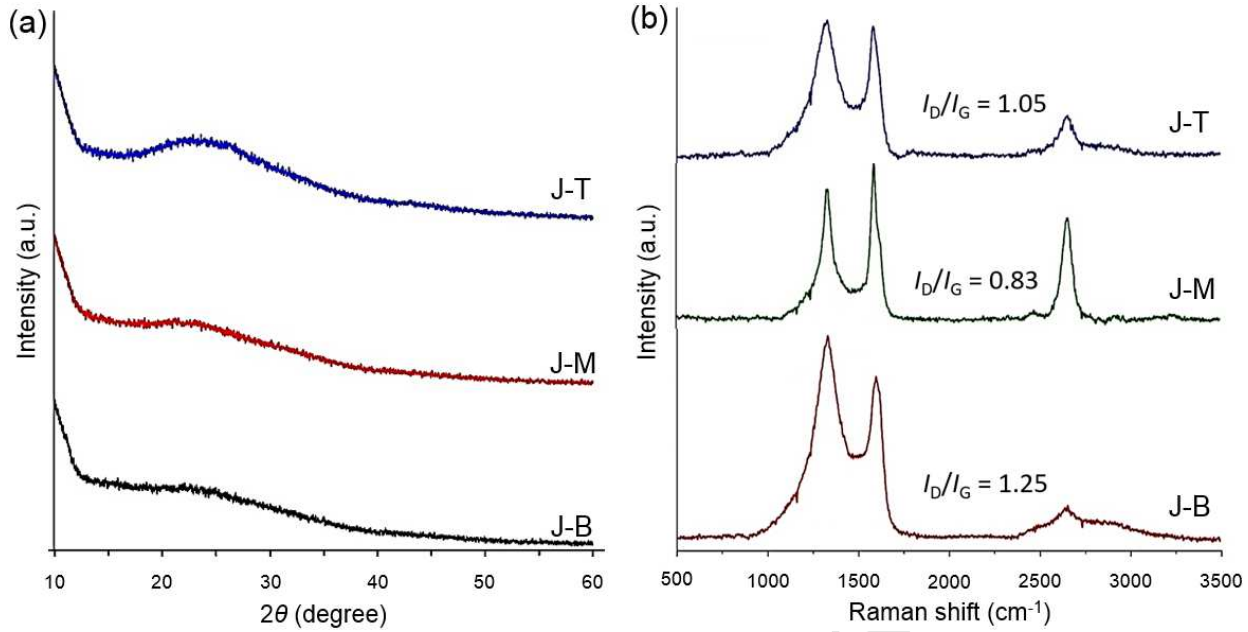

Figure 2. (a) Wide-angle X-ray diffraction patterns and (b) Raman spectra of nanoporous carbons prepared from different parts of the jute fiber.

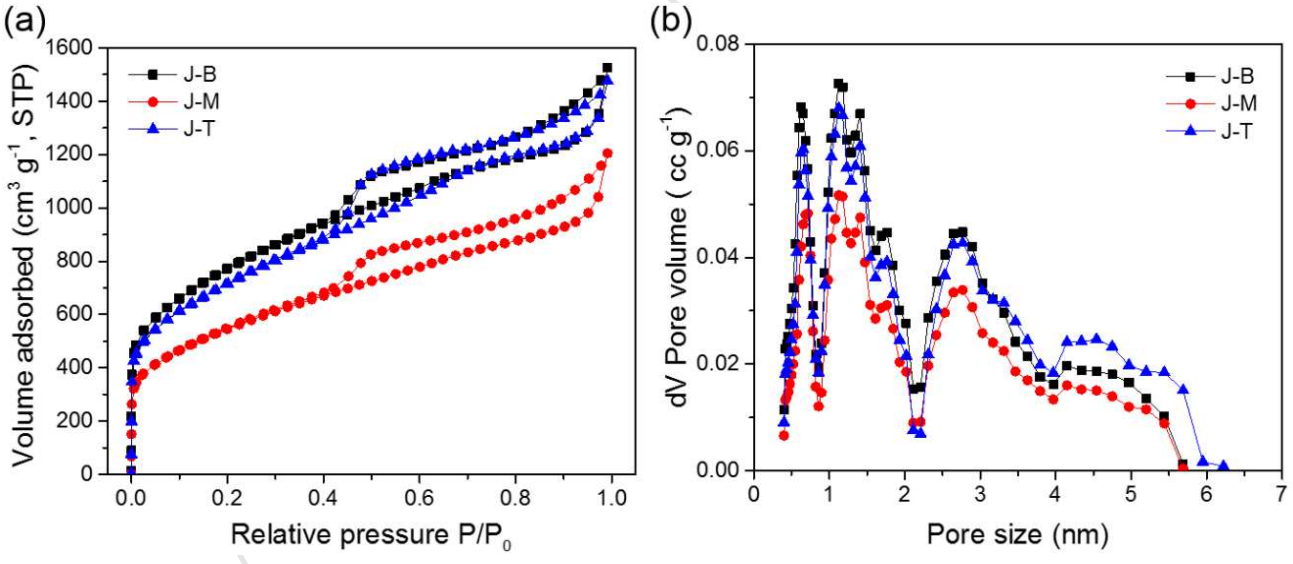

Figure 3. (a) N_2 adsorption-desorption isotherms and (b) pore size distribution curves of nanoporous carbons prepared from different parts of the jute fiber. The DFT method was used to obtain the pore size distribution.

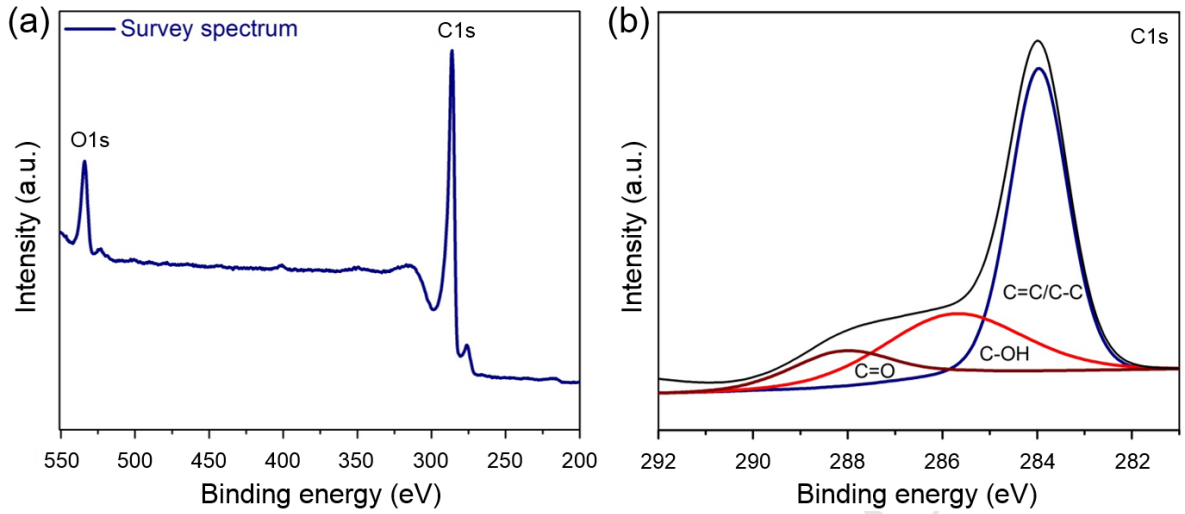

Figure 4. (a) X-ray photoelectron spectroscopy survey spectrum and the (b) C 1s spectrum of the J-B sample.

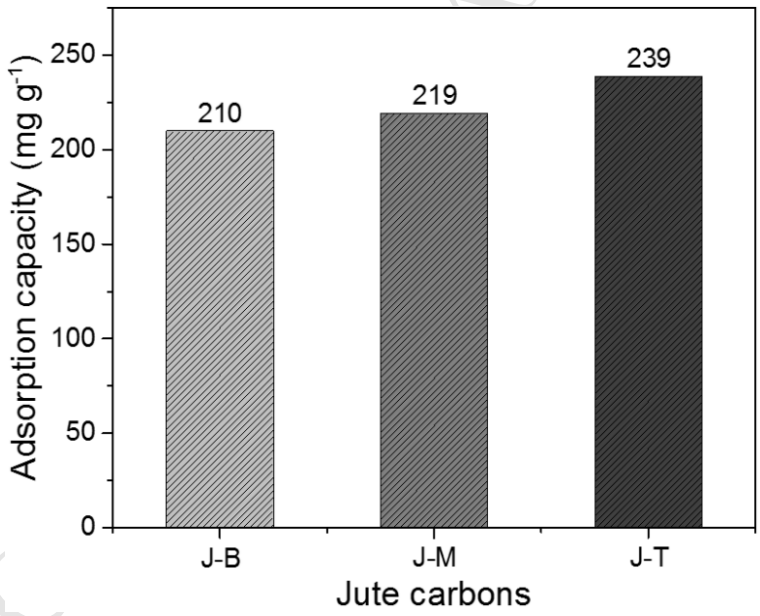

Figure 5. Adsorption of methylene blue by the nanoporous carbons prepared from different parts of the jute fiber.

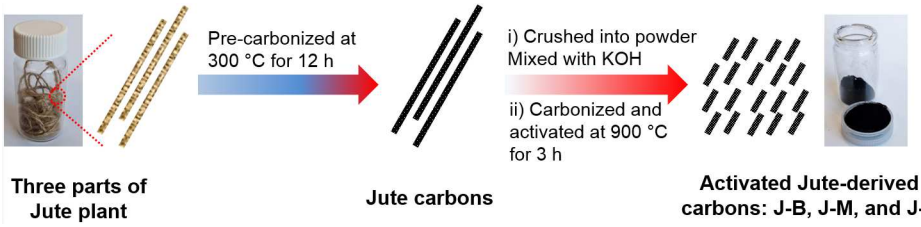

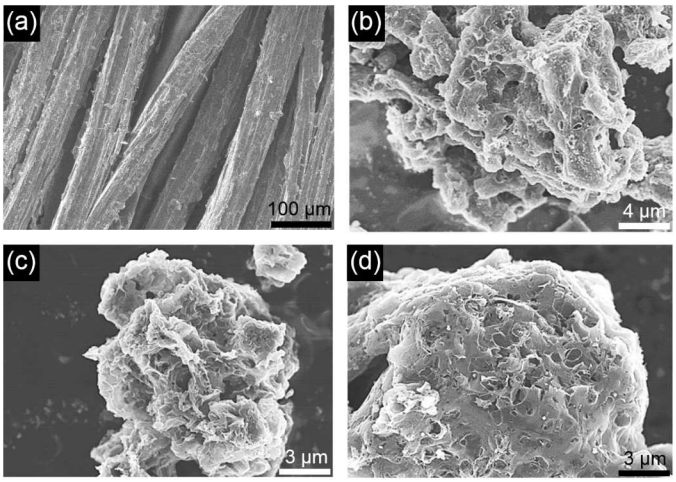

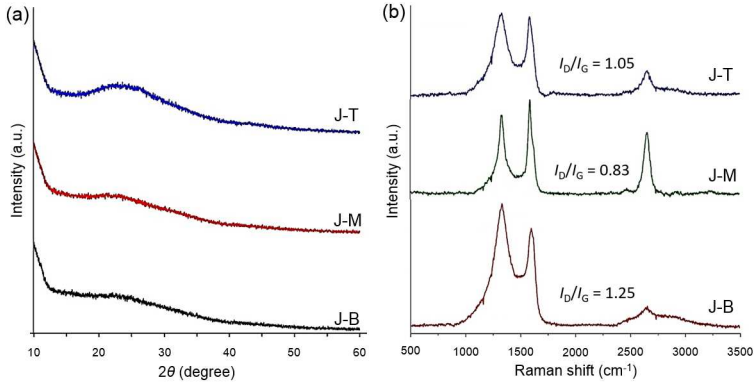

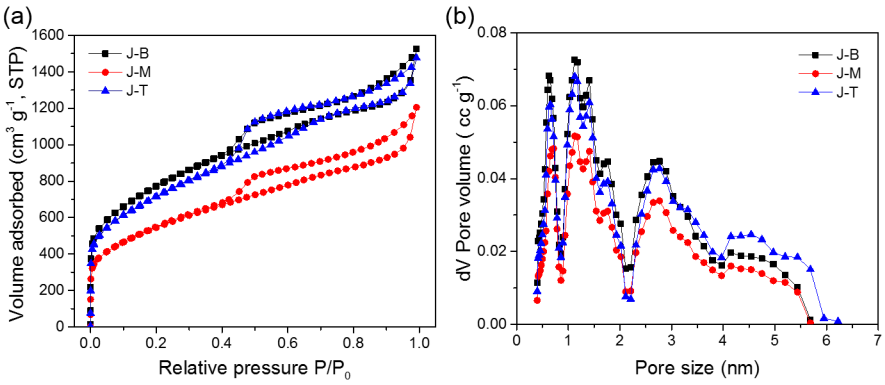

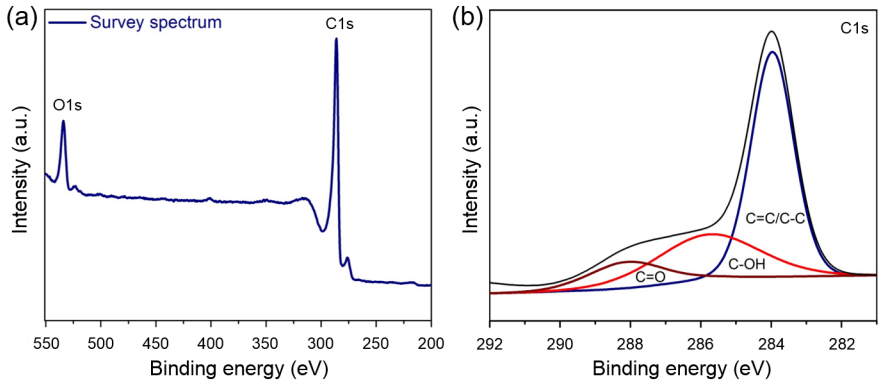

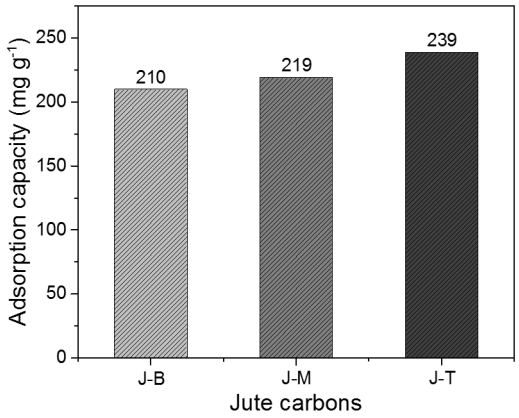

Highlights

- Low cost and renewable biomass, Jute is used for synthesis of nanoporous carbons by chemical activation process with KOH.
- Three different parts of Jute are carbonized and compared for porous properties.
- The NCs prepared from bottom portion of the fiber show high surface area (2682 $m^2 \cdot g^{-1}$) with the presence of both micropores and mesopores.